Nonlinear scattering features of guided waves from fatigue cracks

Yanfeng Shen, Junzhen Wang, Wu Xu

Yanfeng Shen, Junzhen Wang, Wu Xu, "Nonlinear scattering features of guided waves from fatigue cracks ," Proc. SPIE 10600, Health Monitoring of Structural and Biological Systems XII, 106000A (27 March 2018); doi: 10.1117/12.2296413

SPIE.

Event: SPIE Smart Structures and Materials + Nondestructive Evaluation and Health Monitoring, 2018, Denver, Colorado, United States

Nonlinear Scattering Features of Guided Waves from Fatigue Cracks

Yanfeng Shen*[a], Junzhen Wang[a], Wu Xu[b]
[a]University of Michigan-Shanghai Jiao Tong University Joint Institute, Shanghai Jiao Tong University, Shanghai, 200240, China; [b]Department of Aerospace Engineering, Shanghai Jiao Tong University, Shanghai, 200240, China

ABSTRACT

This paper presents the investigation of nonlinear scattering features of guided waves from fatigue cracks. The fatigue cracks nucleated from a rivet hole are studied as the representative case. A small-size numerical model based on the Local Interaction Simulation Approach (LISA) is introduced, which enables the efficient analysis of the Contact Acoustic Nonlinearity (CAN) of guided waves. Fatigue tests on a thin aluminum plate with a rivet hole is conducted to induce cracks in the specimen. An active sensor array surrounding the crack zone is implemented to generate and receive ultrasonic guided waves in various directions. Several distinctive aspects of the nonlinear scattering phenomenon are discussed: (1) the directivity and mode conversion features, which addresses the scattering direction dependence of fundamental and superharmonic wave mode components; (2) the amplitude effect, which stems from the rough crack surface condition with initial openings and closures; (3) the nonlinear resonance phenomenon, which maximizes the nonlinear response during the wave crack interactions at certain excitation frequency ranges. All these features may provide insights and guidelines for nonlinear guided wave based Structural Health Monitoring (SHM) system design. The numerical studies are compared with experimental data. The paper finishes with discussion, concluding remarks, and suggestions for future work.

Keywords: structural health monitoring, nondestructive evaluation, guided waves, nonlinear ultrasonics, scattering, local interaction simulation approach, fatigue cracks, nonlinear resonance

1. INTRODUCTION

Fatigue cracks exist as great menace to engineering structures, because they are barely visible and hard to detect. Thus, the development of effective fatigue crack detection methodologies is of critical importance. Among current solutions, ultrasonic inspection technology has been found to be promising. Compared with linear ultrasonic techniques which are sensitive to gross defects, the nonlinear counterpart, on the other hand, proves to be more sensitive to incipient changes such as fatigue cracks. When guided waves interact with fatigue cracks, Contact Acoustic Nonlinearity (CAN) would arise, which may introduce distinctive signal features, such as sub/super harmonic generation, DC response, mixed frequency modulation response (sideband effects), and various frequency/amplitude dependent threshold behaviors [1]. As a consequence, nonlinear guided wave based inspection techniques are drawing increasing attention among the Structural Health Monitoring (SHM) and Nondestructive Evaluation (NDE) communities, because it inherits both the sensitivity from nonlinear ultrasonics and the large-area inspection capability of guided waves [2].

Many researchers have explored using guided waves for crack detection. Some of them used the linear scattering features. Fromme investigated ultrasonic guided wave scattering for fatigue crack characterization using non-contact measurements [3]. Chan et al. continued this high frequency guided wave laser testing approach to monitor the fatigued crack growth in multi-layer model aerospace structures [4]. Chen et al. utilized a sparse sensor array to estimate the scattering pattern of guided waves from fatigue cracks [5]. To further analyze the scattering of guided waves from a fastener hole with a fatigue crack, Masserey and Fromme conducted both finite difference modeling and experiments with laser interferometer [6]. Quaegebeur et al. proposed an experimental technique to measure the scattering pattern from geometric discontinuities, where they found the scattering pattern from a fatigue crack differed much from that of a machined notch [7]. These research efforts generally focused on the linear scattering features of fatigue cracks, whereas the nonlinear counterpart has also drawn much attention. Klepka et al. adopted the nonlinear acoustics and wave modulation technique to identify fatigue cracks [8]. Utilizing the load-differential effect, Chen et al. took advantage of the crack close status under varying loading conditions to image the fatigue crack [9]. Hong et al. achieved accurate localization of a fatigue crack by the temporal nonlinear signal features [10]. Wu et al. explored using the nonlinear amplitude effect to construct instantaneous baseline

* yanfeng.shen@sjtu.edu.cn, Phone: +86-21-34206524, Fax: +86-21-34206525

Health Monitoring of Structural and Biological Systems XII, edited by Tribikram Kundu, Proc. of SPIE
Vol. 10600, 106000A · © 2018 SPIE · CCC code: 0277-786X/18/$18 · doi: 10.1117/12.2296413

for fatigue crack detection with the tomography imaging algorithm [11]. Liu et al. extracted the fatigue crack information using the noncontact measurements and nonlinear modulation method, which allowed the visualization of fatigue cracks using scanning laser vibrometry [12, 13]. Lim et al. further conducted the study to develop the field application of the baseline free nonlinear ultrasonic modulation approach and successfully detected the fatigue crack [14]. Cheng et al. quantified the fatigue crack using a nonlinear ultrasonic phased array imaging technique and found the nonlinearity of the sensing signals increases with the fatigue crack length [15]. Many modeling methodologies have been developed to investigate nonlinear wave crack interactions [16]. Analytical models are computational efficient and allow fast parametric studies, but they are confined by the complexity of structures and damage types [17]. To fully capture the 3-D nonlinear dynamics, finite element method (FEM) for contact-impact problems has been widely investigated, maturing over the years [18]. Recent development of Local Interaction Simulation Approach (LISA) into the nonlinear region makes it possible to analyze nonlinear interactions between guided waves and fatigue crack in a highly efficient manner [19, 20].

In this study, a small-size LISA model is tailored for the analysis of nonlinear scattering of guided waves at fatigue cracks. The directivity and mode conversion features are discussed for an idealized breathing crack model. Then, the rough crack surface with initial openings and closures is considered and the amplitude effect of the nonlinear scattering will be shown. Finally, the nonlinear resonance phenomenon will be explored using a chirp excitation. Distinctive subharmonic and superharmonic components can be observed at the resonance frequencies. Experiments on an aluminum plate with a rivet hole fatigue crack are conducted and compared with the numerical analysis.

2. SMALL-SIZE LISA MODEL FOR GUIDED WAVE SCATTERING ANALYSIS

LISA is a finite-difference based numerical simulation method. It approximates the partial differential elastodynamic equations with finite difference quotients in the discretized temporal and spatial domains. The final iterative equations (IEs) determine the displacements of a certain node at current time step based on the displacements of its eighteen neighboring nodes at previous two/three time steps, depending on whether material damping is considered. For details of the derivation for the LISA IEs, the readers are referred to Ref. [21]. A penalty method was deployed to introduce contact dynamics into LISA. When the crack surfaces come into contact, contact forces are acted on the contact nodes to constrain the in-contact motion. Thus, the modeling of the alternating boundary condition can be achieved. A Coulomb friction model was integrated to capture the stick-slip contact motion. The details of the contact LISA formulation and the guidelines for the proper choice of computational parameters for an accurate and converged solution are given in Ref [19].

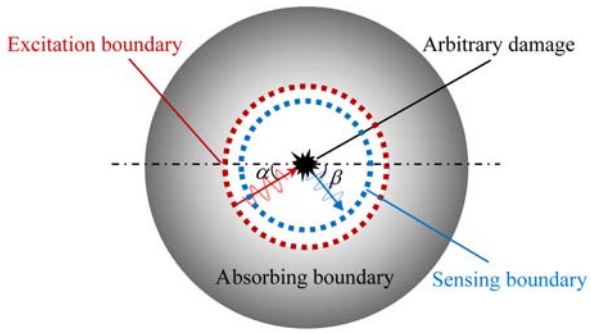

Figure 1: Small-size LISA model for guided wave scattering analysis.

Figure 1 presents the small-size LISA model for guided wave scattering analysis. The model is comprised of an interior region with the damage at the center and an exterior region extended with absorbing layers. Since LISA belongs to the family of numerical methods with spatial and temporal discretization, such model is capable of describing arbitrary damage profiles. The red circle represents the exciting points where guided waves can be generated from an arbitrary incident angle. The blue circle layouts the sensing points picking up the scattered waves in each direction. The absorbing boundary is implemented using the Absorbing Layers with Increasing Damping (ALID) method [22]. It allows the simulation of wave propagation in an infinite domain with a finite size model. The guided waves directly generated by the excitation points and those scattered by the damage are absorbed by the silent boundary setup.

Single mode guided waves are generated at the excitation points by exerting in-phase or out-of-phase traction forces at the top and bottom surfaces of the plate. The contact problem is solved using the transient dynamic analysis. A continuous harmonic excitation is gradually introduced into the model to generate guided waves at the frequency of interest. Guided waves will impinge on the damage and nonlinear interactions may take place. Scattering and mode conversion will happen

as well. The scattered waves will radiate outward and be picked up by the sensing points and finally absorbed by the ALID boundary. In order to perform the quantitative analysis of the nonlinear scattering features, the sensing points across the plate thickness are all employed. The motion of the points across the thickness allows the decomposition of the guided waves modes. In this way, the model allows the extraction of the wave modes in the scattered wave field quantitatively. This conference paper mainly focuses on presenting the results of our findings, whereas the details of the extraction procedure can be found in Ref. [23].

There are two aspects that make this model computationally efficient: (1) the size of the model is minimized by employing the absorbing boundary, which considerably alleviates the computational burden; (2) the LISA model is implemented using the Compute Unified Device Architecture (CUDA) technology and executed massively in parallel on powerful graphics cards, which facilitates the high performance in computing. Both factors contributes to the high computational efficiency of the small-size LISA model.

3. EXPERIMENTS ON WAVE CRACK NONLINEAR INTERACTIONS

In addition to the modeling efforts, guided wave active sensing experiments on a fatigue specimen were carried out. Figure 2 shows the specimens used for the investigation. In order to demonstrate the nonlinear effects caused by the nonlinear interactions between guided waves and the fatigue crack, an aluminum plate with a pristine rivet hole was also prepared as the comparative set. Both specimens were machined from a 1-mm thick 2024 aluminum plate. A 4-mm diameter rivet hole was machined on both plates. One of the plates was loaded using the fatigue test facility. The fatigue specimen was subjected to a total number of 350,000 cycles with load control. The fatigue cracks were nucleated from two sides of the rivet hole and grow outwards. A 30-mm long fatigue crack was finally obtained on each side of the hole. On the pristine plate, a pair of Piezoelectric Wafer Active Sensors (PWAS) were bonded, forming a pitch-catch active sensing configuration. On the fatigued plate, a circle of 24 PWAS transducers were mounted as a sensor array to generate and receive guided waves at every 15° angle. Damping clay was implemented surrounding the active sensing area to absorb boundary reflections.

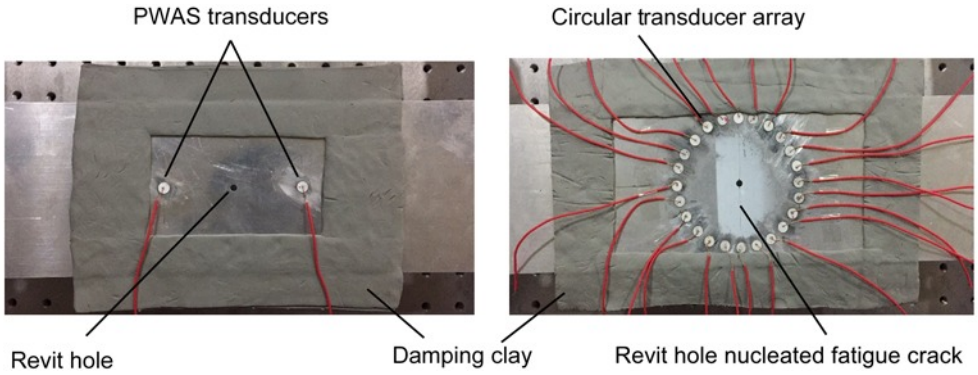

Figure 2: Specimens for the ultrasonic active sensing tests: (a) aluminum plate with a pristine rivet hole; (b) aluminum plate with rivet hole fatigue cracks.

Figure 3 presents the experimental setup for the nonlinear ultrasonic tests. A Keysight 33500B arbitrary function generator was used to generate excitation waveforms. The excitation signal was further amplified by a Krohn-hite 7602M wideband power amplifier and was applied on the transmitter PWAS. Guided waves were generated, propagated along the plate, interacted with the crack, and are finally picked up by the receiver PWAS. The sensing waveforms were collected by the Keysight DSO-X 3014T digital storage oscilloscope. Using the circular sensor array, guided waves can be emitted by various incident angles. While one PWAS was used as the transmitter, all the other transducers performed as sensors, recording the structural response. Thus, the scattered information can be obtained in every 15° direction. Since the frequency domain information is of interest for the nonlinear ultrasonic study, excitations with a large number of counts are desired to obtain high resolution frequency domain details. In the experiments, continuous harmonic excitations were used. Comparative study between the pristine rivet hole and the fatigued rivet hole plates were first conducted. Then, the amplitude effect in the nonlinear ultrasonic inspections were investigated by applying various levels of excitation signals. Finally, to investigate the possible nonlinear resonance effect, frequency sweeping experiments were carried out. The experimental data and its comparison with the numerical analysis will be shown in the following section.

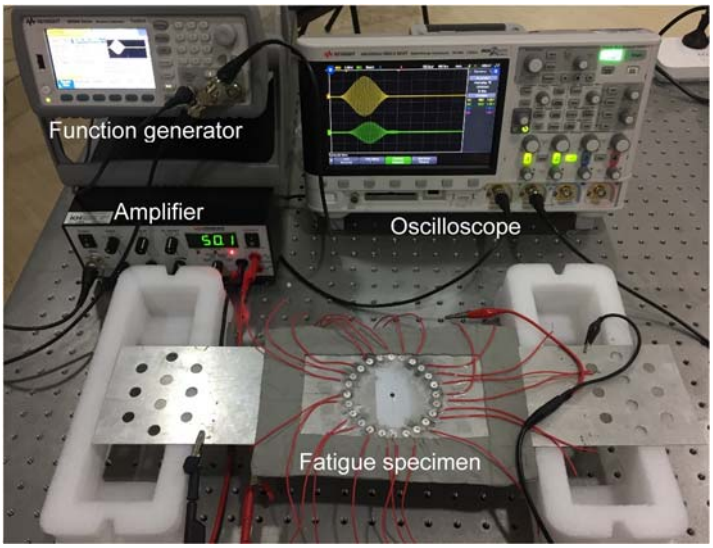

Figure 3: Experimental setup for the nonlinear ultrasonic tests.

4. SCATTERING OF GUIDED WAVES FROM RIVET HOLE FATIGE CRACKS

This section presents our numerical and experimental results on the nonlinear scattering features of guided waves from a rivet hole fatigue crack. The directivity and mode conversion features of the scattering phenomenon will first be illustrated using an idealized breathing crack model. Then, the rough crack surface condition with initial openings and closures will be considered to discuss the amplitude effect during the nonlinear scattering procedure. Finally, the nonlinear resonance effects will be discussed.

4.1 Directivity and mode conversion features of nonlinear scattering

Our analysis starts with the idealized breathing crack model, where the crack surfaces are considered to be smooth in perfect touching-contact condition without initial gap nor pre-stresses. Figure 4 presents the numerical simulation results of nonlinear interaction between the fundamental Lamb wave modes with the rivet hole fatigue crack at 100 kHz using the small-size LISA model. Figure 4a shows the generation of S0 wave mode and its interaction with the fatigue crack by opening it up. While the compressional part of the wave will close the crack surfaces as shown in Figure 4b. The high wave amplitude induced by the impact between the crack interfaces can be clearly noticed. The nonlinearity of the wave crack interactions arises from the periodic local stiffness change through the crack open and close contact dynamic procedure. Figure 4c and Figure 4d show the generation of short-wavelength A0 Lamb mode into the structure and its interaction with the crack. Due to the antisymmetric motion of A0 mode across the plate thickness, the top and bottom crack surface will be opened and closed, taking turns in an alternative manner. It can also be noticed that the guided waves generated and scattered are effectively absorbed by the ALID boundary.

In order to evaluate the nonlinear scattering phenomenon, the scattering coefficients were extracted using modal decomposition technique based on guided wave mode shapes calculated from the Semi-Analytical Finite Element (SAFE) method. The Wave Damage Interaction Coefficients (WDICs) were adopted to quantify the participation of each guided wave mode during the scattering procedure. A typical WDIC can be expressed as $C_{A-B}(\alpha, \beta, f_n)$. Two sub-indices were used to represent the scattering and mode conversion effects. The sub index A represents the incident wave mode, while B represents the scattered wave mode. α and β stand for the incident and scattering angles. f_n denote the scattered frequency component of interest corresponding to the fundament excitation, second, third, or even higher superhamrmonics. For instance, if the incident wave frequency is at 100 kHz, then $C_{S0-A0}(30,150,200)$ means the second harmonic frequency (200 kHz) scattering coefficient of mode converted A0 waves in 150° direction from an oblique 30° S0 incident wave; $C_{A0-SHS0}(0,180,300)$ is the scattering coefficient of mode converted fundamental symmetric shear horizontal mode (SHS0) at the third harmonic in 180° direction due to the 0° incident A0 mode incidence at the damage. Details about the definition and derivation of WDICs can be found in Refs. [23, 24].

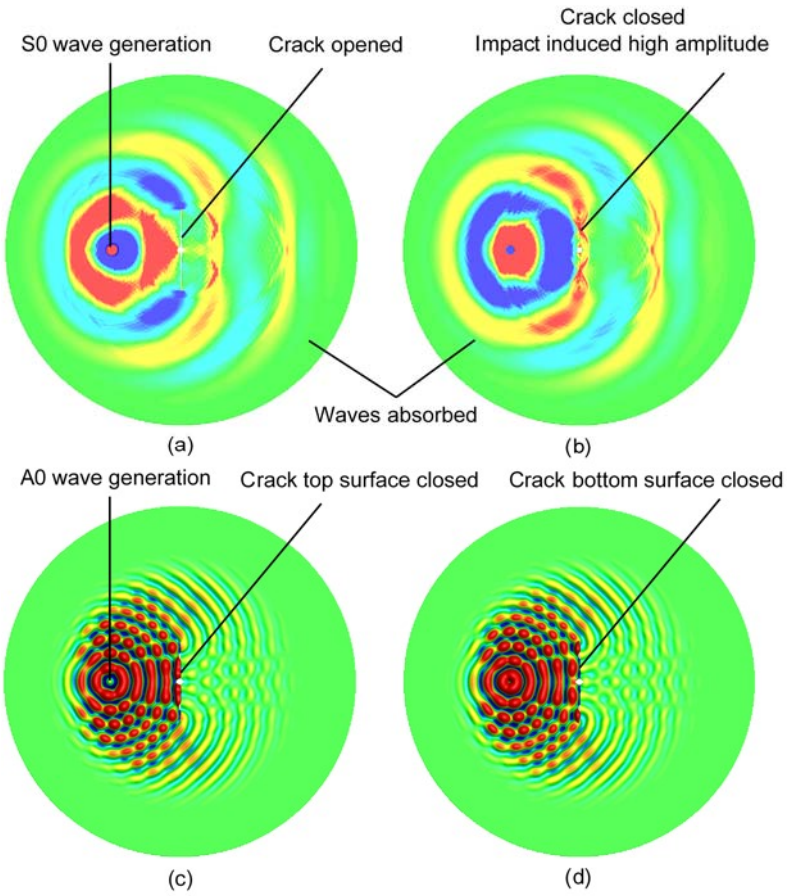

Figure 4: Numerical simulation of nonlinear interactions between fundamental Lamb wave modes with the rivet hole fatigue crack at 100 kHz using the small-size LISA model: (a) S0 wave opens the fatigue crack; (b) S0 wave closes the fatigue crack with impact induced high amplitude; (c) A0 wave closes the top surface of the crack; (d) A0 wave closes the bottom surface of the crack.

Figure 5 presents the scattering coefficients for the case of S0 wave incidence at the rivet hole fatigue crack. At the fundamental frequency of 100 kHz, the S0 incident waves were scattered as S0 mode and converted to SHS0 mode. No antisymmetric A0 Lamb mode was converted during the nonlinear scattering procedure. Similar mode conversion effect can be noticed for the second and the third harmonic scattering coefficients, i.e., when S0 wave interact with an idealized breathing crack, mode conversion only happened between the symmetric modes (S0 and SHS0) and the antisymmetric mode would not participate in the scattering procedure. Another important feature is the direction dependence of the scattering amplitude. At the fundamental frequency, the largest amplitude of scattered SHS0 mode happened around 30^{o} and 150^{o}, while the scattered S0 possessed the high amplitudes in 0^{o} and 180^{o} perpendicular to the crack line orientation. At the second and third higher harmonic frequencies, however, the scattered S0 mode showed its highest forward amplitude in 30^{o} and 15^{o} directions respectively.

When A0 mode impinged on the fatigue crack, the scattering pattern showed totally different behavior. Figure 6 shows that all the possible wave modes participated in the scattering procedure. At the fundamental frequency, the majority of the wave energy was scattered as A0 mode. Only a very small amount was converted to SHS0 and S0 modes. Nevertheless, the second harmonic frequency involved much less participation from A0, while SHS0 and S0 mode scattering amplitude gained much larger amplitude. This indicates that the principal energy concentrated on the symmetric modes due to the mode conversion. Further, at the third harmonic frequency, A0 mode takes the majority of the scattering energy again, while the symmetric modes amplitude dropped significantly. Thus, the mode conversion pattern showed an alternating pattern between the antisymmetric and symmetric modes by taking up the principal scattering energy. Such alternating mode conversion feature is particularly special and will only happen during the nonlinear scattering procedure. The linear interaction between guided waves and a notch would not possess such distinctive mode conversion features.

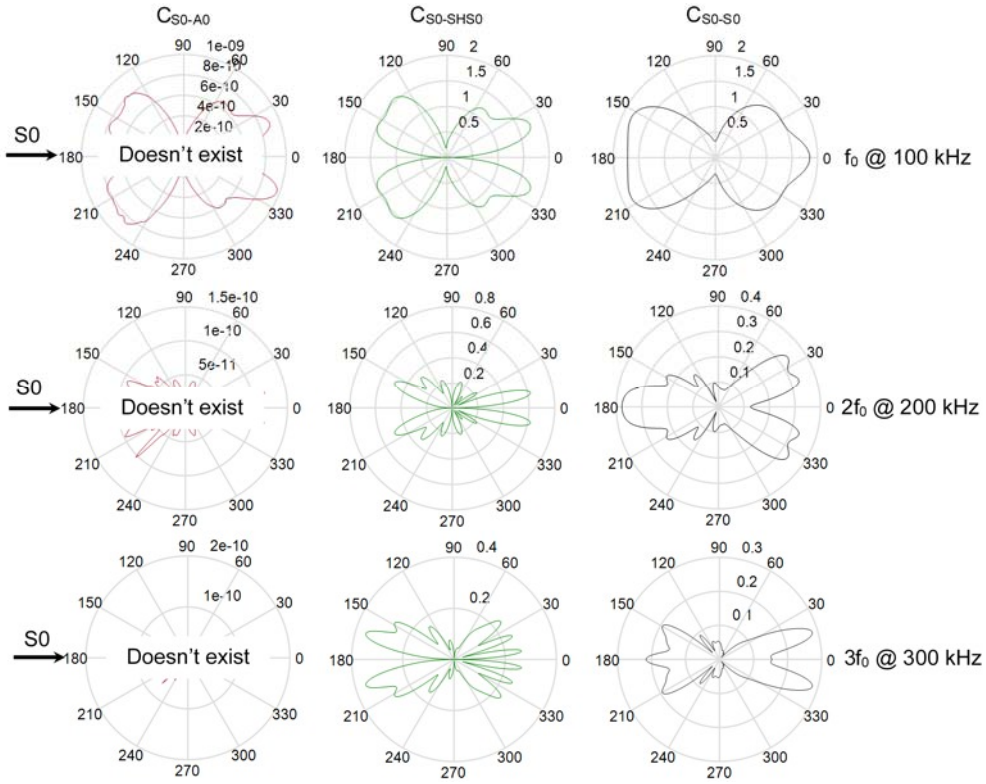

Figure 5: Scattering coefficients at the fundamental and superharmonic frequencies of incident S0 wave mode at 100 kHz.

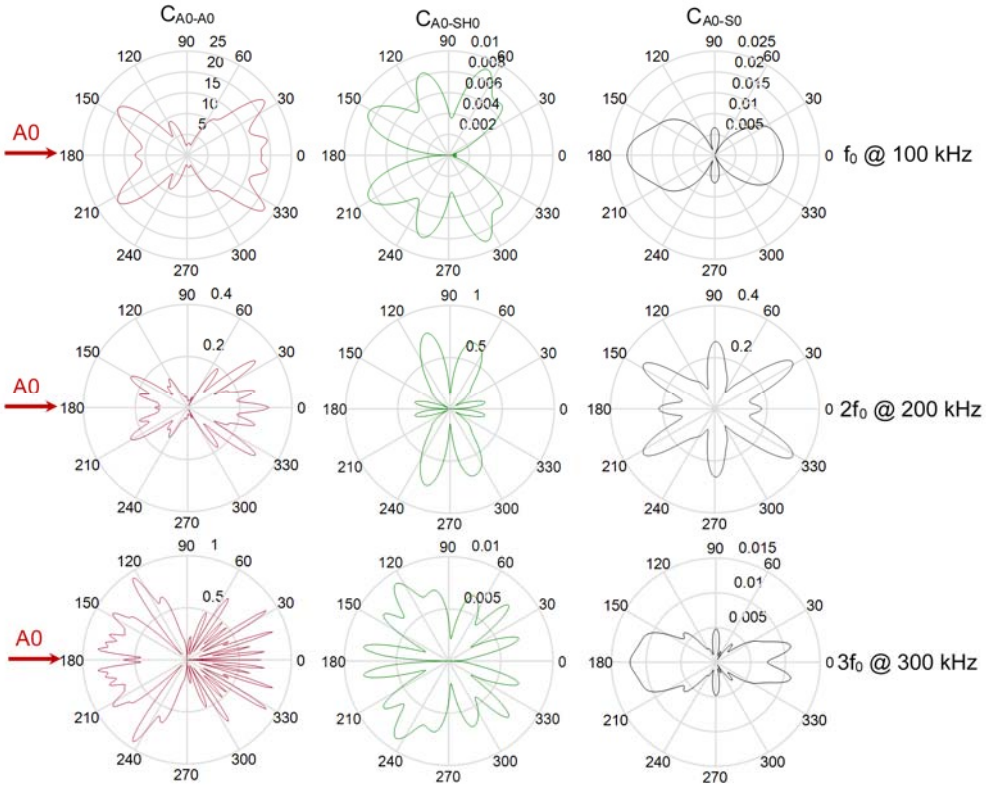

Figure 6: Scattering coefficients at the fundamental and superharmonic frequencies of incident A0 wave mode at 100 kHz.

4.2 Amplitude effect of nonlinear scattering

The analysis presented in the previous subsection is based on the assumption of an idealized breathing crack: the crack surfaces are smooth and in perfect contact condition with no pre-stresses nor initial gaps. However, a real fatigue crack surface differs much from this idealized assumption. Such deviation may bring uncertainties and variation into the scattering procedure. Figure 7a shows the microscopic image of a typical fatigue crack in aluminum. It can be observed that the crack surface is rough with a zigzag crack trace. At certain location, relatively large material voids can be seen, while at others the distance between the crack interfaces are much closer. Within the rough crack surface, initially closed areas also exist, indicating pre-stressed contact points. The initial openings and closures are distributed along the crack surface in a relatively random patter. In order to capture the nature of such rough crack surfaces, randomly distributed initial gap functions were adopted for the contact pairs in the LISA model. Figure 7b presents the randomly generated initial openings and closures along the crack contact surfaces following a normal distribution. A positive gap distance represents the initial openings and the negative gap distances corresponds to the initial closures with pre-stresses. The rough crack surface condition gives rise to the amplitude effect in nonlinear scatterings.

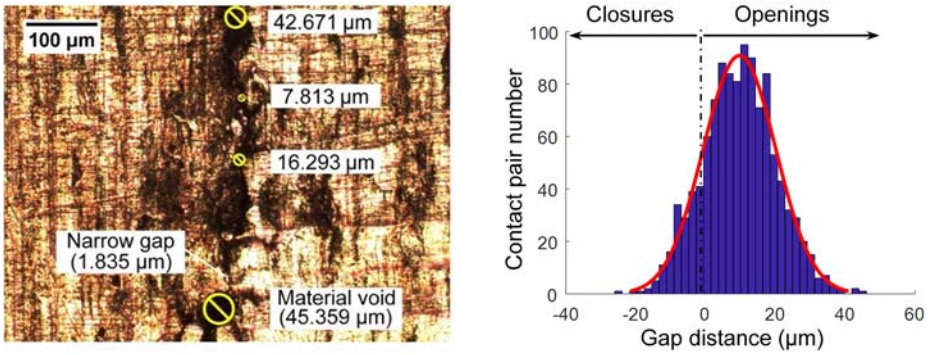

(a) (b)

Figure 7; (a) Microscopic image of a typical fatigue crack; (2) assumed normal distribution of initial openings and closures at the rough crack interface.

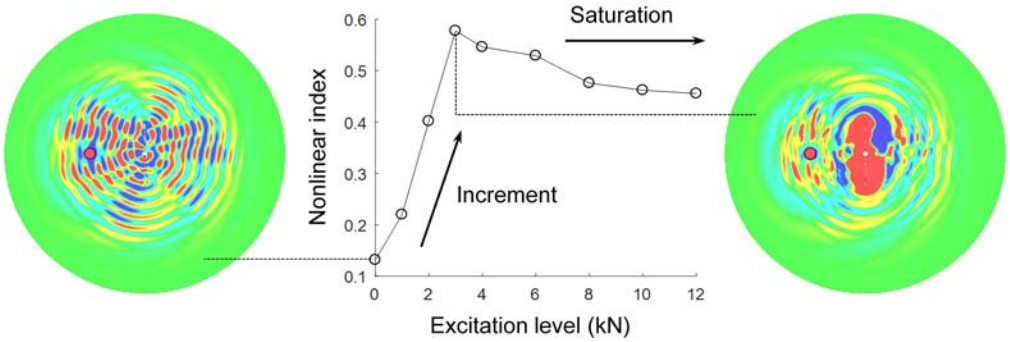

Figure 8: Relationship between nonlinearity index and excitation amplitude and the amplitude dependent scattering patterns.

Figure 8 presents the excitation amplitude influence on the ultrasonic guided wave scattering. The nonlinear index based on the ratio of harmonic frequency amplitudes is plotted against the excitation level. When the excitation amplitude is low, the nonlinearity in the scattered waves is very weak. With an increasing excitation amplitude, the nonlinearity of the wave field undergoes substantial increment. Beyond a certain level, the nonlinearity saturated and plateaued. This is because at low excitation level, only a small fraction of the contact pairs participated in the contact dynamic procedure. With larger excitation amplitudes, more and more contact pairs will be engaged in the crack surface nonlinear interactions. The numerical simulated wave field are also plotted in Figure 8. Both cases correspond to the S0 wave incident situation. However, the results differs much from those shown in Figure 4a and Figure 4b. One obvious difference is that the scattered wave field now contains short wavelength A0 mode, indicating the mode conversion from S0 mode into A0 mode during the wave crack interactions. A second difference is that the scattering field becomes asymmetric or skewed. And the third difference is that at different excitation levels, the scattering patterns look totally different, i.e., the excitation amplitude

changes the scattering feature. Such nonlinear amplitude influence may lay the foundation for a class of nonlinear ultrasonic SHM technique based on the amplitude dependent response.

4.3 Nonlinear resonance during wave crack interactions

In addition to the directivity, mode conversion, and amplitude effects of nonlinear ultrasonic scattering, another important and special feature is the nonlinear resonance during wave crack interactions. At different excitation frequencies, the nonlinear response may vary much from each other. Within a certain frequency range, nonlinear superharmonic resonances may be much stronger, while within others the nonlinear higher harmonics can hardly be observed. In addtion, the subharmonic resonances are more sensitive to the excitation frequency.

In order to investigate the nonlinear resonance phenomena, a frequency sweeping test was carried out using our small-size LISA model. The excitation frequency was swept from 50 kHz up to 300 kHz. Figure 9a presents the in-plane displacement 50 mm behind the fatigue crack. The zigzag nonlinear response pattern can be clearly noticed in the time trace. After performing the shot-time Fourier transform, the time-frequency component of the signal was further revealed. Figure 9b shows that in addition to the fundamental frequency ramping up with time, DC component and superharmonic resonances also showed up. It should be noted that the amplitude of the superharmonics are not constant throughout the frequency range, possessing humps and valleys, indicating the resonance phenomenon. A special subharmonic resonance can also be observed around 160 μs, corresponding to approximately 180 to 190 kHz. The subharmonic resonance is very sensitive to the excitation frequency and the local resonant frequency of the damage itself.

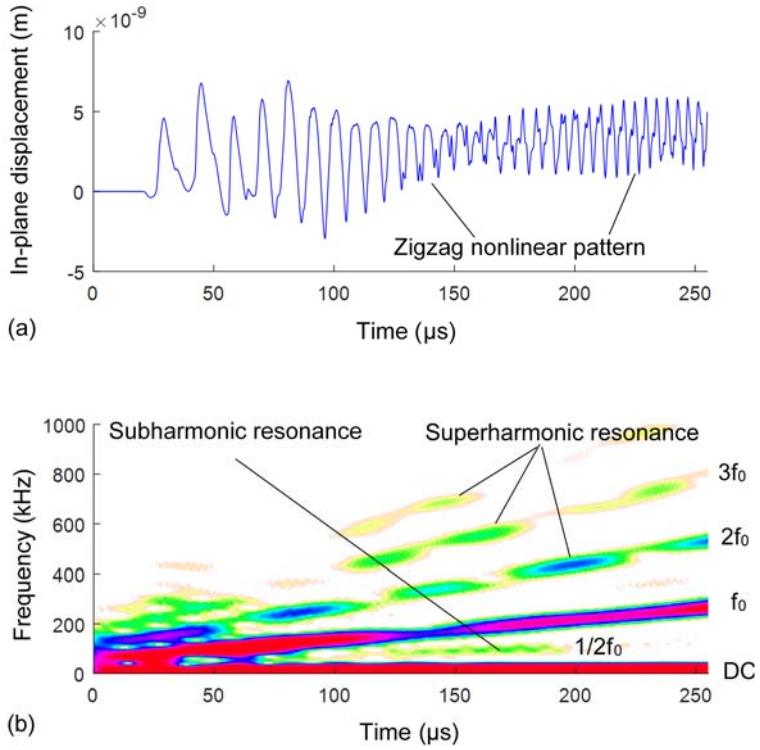

Figure 9: Frequency sweeping results of nonlinear subharmonic and superharmonic resonances using the numerical model.

The frequency sweeping experiments on the fatigue specimen were also performed. Figure 10a shows the experimental result when a 5 Vpp excitation amplitude was used. It can be seen that only the fundamental excitation frequency component was present. Figure 10b shows the frequency sweeping result under a 50 Vpp excitation. Distinctive superharmonics can be clearly noticed. The superharmonic component also showed similar resonant behavior as predicted by our numerical analysis. The subharmonic resonance did not show as obvious as in the numerical results. In addition, the resonant frequencies also do not match exactly between experiments and our model. This is due to the fact that the microscopic rough feature of the crack interfaces will influence the dynamic behavior of the crack. The excitation amplitude would further affect the nonlinear response. However, the numerical analysis is much indicative and can provide insights to understanding the physical phenomena.

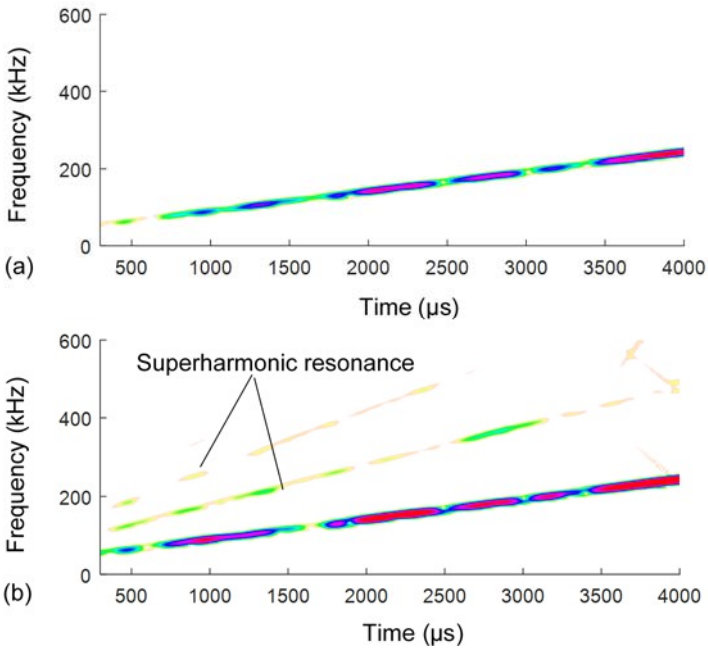

Figure 10: Experimental results of frequency sweeping tests: (a) time-frequency spectrum under 5 Vpp excitation; (b) time-frequency spectrum under 50 Vpp excitation.

To present the existence of subharmonic resonance as the model prediction, experiments on the fatigue specimen were performed by applying a 50 Vpp continuous harmonic excitation between 180 kHz and 190 kHz. Around 185 kHz, the subharmonic resonance was observed. Figure 11a shows the frequency component of the excitation, containing only the excitation frequency at 185.2 kHz. Figure 11b presents the frequency-domain response after the wave crack interaction. In addition to the fundamental frequency at f_0 = 185.2 kHz, the subharmonic component around 93.27 kHz was also clearly shown. Sideband frequency component at f_0 + 1/2 f_0 showed up as well due to the mixed frequency response or the so-called wave modulation. Superharmonics also appeared at $2f_0$, $3f_0$, etc. It should be pointed out that in the experiment, the existence condition for the subharmonic resonance is quite demanding. The excitation frequency and amplitude matching condition must be satisfied.

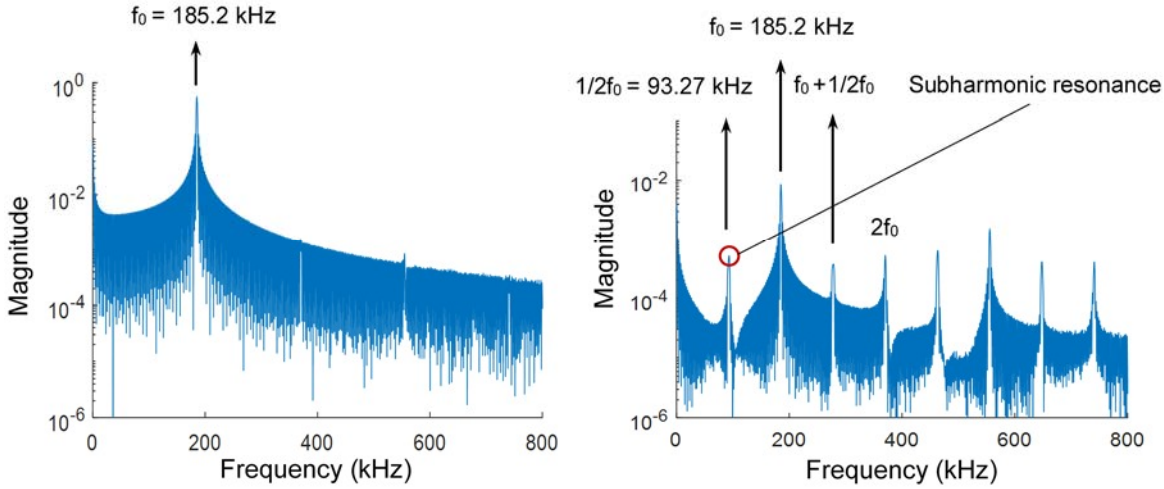

Figure 11: Subharmonic resonance spectrum at 185.2 kHz: (a) excitation containing only the fundamental frequency; (b) nonlinear response with subharmonic, sideband, and superharmonic resonances.

5. CONCLUDING REMARKS

This paper presented the investigation of nonlinear scattering features of guided waves from rivet hole fatigue cracks. A small-size LISA model was tailored for efficient analysis of the scattering procedure. Active sensing experiments were performed to study the nonlinear features during wave crack interactions. Several distinctive aspects of the nonlinear scattering phenomenon were discussed: (1) the directivity and mode conversion features; (2) the amplitude effect; (3) the nonlinear resonance phenomenon.

Our investigation started with the idealized breathing crack model. Quantitative analysis was conducted and the scattering coefficients were obtained. It was found that the incident S0 mode would only be scattered as symmetric modes (S0 and SHS0). No A0 waves were present in the scattered wave field. When A0 mode impinged on the fatigue crack, all the possible wave modes would participate in the scattering procedure. However, it showed a special alternating participation phenomenon between the antisymmetric and symmetric modes. Next, the rough crack surface model was used to show the amplitude effect and random feature during the ultrasonic nonlinear scattering procedure. The analysis showed that the nonlinearity of the guided waves grew with the increasing excitation amplitude. The scattering patterns also showed skewed shapes which also differed from each other under various excitation amplitudes. Finally, the nonlinear resonance phenomenon was investigated by conducting the frequency sweeping tests using both the numerical model and the experiments. It was found that superharmonic and subharmonic resonances exist at various frequency ranges. The experiment showed that the resonances were also amplitude dependent. In addition, the existence condition for the subharmonic resonance was quite demanding. The excitation frequency and amplitude matching condition must be satisfied. All these special features of nonlinear ultrasonic scattering may provide insights and guidelines for nonlinear guided wave based SHM system design.

For future work, nonlinear guided wave SHM methods should be explored based on the special features of the nonlinear scattering procedure, such as amplitude based technique, nonlinear resonance spectrum technique, and the visual based nonlinear laser imaging methods.

ACKNOWLEDGEMENTS

The support from the National Natural Science Foundation of China (contract number 51605284) is thankfully acknowledged.

REFERENCES

[1] Z. Su, C. Zhou, M. Hong, L. Cheng, Q. Wang and X. Qing, "Acousto-ultrasonics-based fatigue damage characterization: linear versus nonlinear signal features," *Mechanical Systems and Signal Processing,* vol. 45, no. 1, pp. 225-239, 2014.

[2] D. Dutta, H. Sohn, K. A. Harries and P. Rizzo, "A nonlinear acoustic technique for crack detection in metallic structures," *Strctural Health Monitoring, An International Journal,* vol. 8, no. 3, pp. 251-262, 2009.

[3] P. Fromme, "Noncontact measurement of guided ultrasonic wave scattering for fatigue crack characterization," in *SPIE Smart Structures and NDE*, San Diego, 2013.

[4] H. Chan, B. Masserey and P. Fromme, "High frequency guided ultrasonic waves for hidden fatigue crack growth monitoring in multi-layer model aerospace structures," *Smart Materials and Structures,* vol. 24, pp. 1-10, 2015.

[5] X. Chen, J. E. Michaels and T. E. Michaels, "A Methodology for Estimating Guided Wave Scattering Patterns From Sparse Transducer Array Measurements," *IEEE Transactions on Ultrasonics, Ferroelectrics, and Frequency Control,* vol. 62, no. 1, pp. 208-219, 2015.

[6] B. Masserey and P. Fromme, "Analysis of high frequency guided wave scattering at a fastener hole with a view to fatigue crack detection," *Ultrasonics,* vol. 76, no. 1, pp. 78-86, 2017.

[7] N. Quaegebeur, N. Bouslama, M. Bilodeau, R. Guitel, P. Masson, A. Maslouhi and P. Micheau, "Guided wave scattering by geometrical change or damage: Application to characterization of fatigue crack and machined notch," *Ultrasonics,* vol. 73, no. 1, pp. 187-195, 2017.

[8] A. Klepka, W. Staszewski, R. Jenal, M. Szwedo, J. Iwaniec and T. Uhl, "Nonlinear acoustics for fatigue crack detection – experimental investigations of vibro-acoustic wave modulations," *Structural Health Monitoring - An International Journal,* vol. 11, no. 2, pp. 197-211, 2011.

[9] X. Chen, J. Michaels, S. Lee and T. Michaels, "Load-differentialimagingfordetectionandlocalizationoffatiguecracks using Lambwaves," *NDT&E International,* vol. 51, no. 1, pp. 142-149, 2012.

[10] M. Hong, Z. Su, Y. Lu, H. Sohn and X. Qing, "Locating fatigue damage using temporal signal features of nonlinear Lamb waves," *Mechanical Systems and Signal Processing,* vol. 60, p. 182–197, 2015.

[11] W. Wu, W. Qu, L. Xiao and D. Inman, "Detection and localization of fatigue crack with nonlinear instantaneous baseline," *Journal of Intelligent Material Systems and Structures,* vol. 27, no. 12, p. 1577–1583, 2016.

[12] P. Liu, H. Sohn and B. Park, "Baseline-free damage visualization using noncontact laser nonlinear ultrasonics and state space geometrical changes," *Smart Materials and Structures,* vol. 24, pp. 1-13, 2015.

[13] P. Liu, H. Sohn, S. Yang and H. Lim, "Baseline-free fatigue crack detection based on spectral correlation and nonlinear wave modulation," *Smart Materials and Structures,* vol. 25, pp. 1-12, 2016.

[14] H. Lim, Y. Kim, G. Koo, S. Yang, H. Sohn, I. Bae and J. Jang, "Development and field application of nonlinear ultrasonic modulation technique for fatigue crack detection without reference data from an intact condition," *Smart Materials and Structures,* vol. 25, pp. 1-14, 2016.

[15] J. Cheng, J. Potter, A. Croxfold and B. Drinkwater, "Monitoring fatigue crack growth using nonlinear ultrasonic phased array imaging," *Smart Materials and Structures,* vol. 26, pp. 1-10, 2017.

[16] D. Broda, W. Staszewski, A. Martowicz, T. Uhl and V. Silberschmidt, "Modelling of nonlinear crack–wave interactions for damage detection based on ultrasound—A review," *Journal of Sound and Vibration,* vol. 333, p. 1097–1118, 2014.

[17] Y. Shen and V. Giurgiutiu, "WaveFormRevealer: An analytical framework and predictive tool for the simulation of multi-modal guided wave propagation and interaction with damage," *Structural Health Monitoring: An International Journal,* vol. 13, no. 5, pp. 491-511, 2014.

[18] Y. Shen and V. Giurgiutiu, "Predictive modeling of nonlinear wave propagation for structural health monitoring with piezoelectric wafer active sensors," *Journal of Intelligent Material Systems and Structures,* vol. 25, no. 4, pp. 506-520, 2013.

[19] Y. Shen and C.E.S. Cesnik, "Modeling of nonlinear interactions between guided waves and fatigue cracks using local interaction simulation approach," *Ultrasonics,* vol. 74, pp. 106-123, 2017.

[20] Y. Shen and C.E.S. Cesnik, "Local interaction simulation approach for efficient modeling of linear and nonlinear ultrasonic guided wave active sensing of complex structures," *Journal of Nondestructive Evaluation, Diagnostics and Prognostics of Engineering Systems,* vol. 1, no. 1, pp. 1-9, 2018.

[21] K. Nadella and C.E.S. Cesnik, "Local interaction simulation approach for modeling wave propagation in composite structures," *CEAS Aeronautical Journal,* vol. 4, no. 1, pp. 35-48, 2013.

[22] Y. Shen and V. Giurgiutiu, "Effective non-reflective boundary for Lamb waves: Theory, finite element implementation, and applications," *Wave Motion,* vol. 58, pp. 22-41, 2015.

[23] Y. Shen and C.E.S. Cesnik, "Efficient Modeling of Nonlinear Scattering of Ultrasonic Guided Waves From Fatigue Cracks Using Local Interaction Simulation Approach," in *ASME 2016 International Mechanical Engineering Congress and Exposition*, Phoenix, Arizona, 2016.

[24] Y. Shen and V. Giurgiutiu, "Combined analytical FEM approach for efficient simulation of Lamb wave damage detection," *Ultrasonics,* vol. 69, pp. 116-128, 2016.